

# Development of high-power and high-energy 2 $\mu\text{m}$ bulk solid-state lasers and amplifiers

Wayne Koen\*, Cobus Jacobs, Lorinda Wu, and Hencharl Strauss  
CSIR National Laser Centre, PO Box 395, Pretoria, South Africa, 0001

## ABSTRACT

A selection of 2  $\mu\text{m}$  lasers and amplifiers developed at the CSIR National Laser Centre in South Africa is presented. A diverse range of near diffraction-limited 2  $\mu\text{m}$  lasers and amplifiers were developed which varied from high-energy, single-frequency oscillators and amplifiers, to compact and efficient MOPA systems delivering high average powers. This was made possible by exploiting various advantageous properties of holmium-doped YLF while mitigating its detrimental properties through the use of novel pump and laser design approaches.

**Keywords:** mid-infrared, laser, amplifier, holmium, thulium, YLF, single-frequency

## 1. INTRODUCTION

Laser sources in the near-infrared region (0.8-1.4  $\mu\text{m}$ ) gained significant market representation in the last quarter of the previous century with the proliferation of both neodymium solid-state lasers as well as diode lasers. Mid-infrared laser sources in the 2-5  $\mu\text{m}$  region, however, lagged behind in both power and availability. Even though they were demonstrated soon after the first laser was developed, significant improvement was required for their use to become more mainstream [1–3].

Sufficient progress has since been made such that mid-infrared lasers are now used, and are considered for use, in several industries. The output wavelengths of these lasers potentially allow processing of materials that do not react in a desirable fashion to traditionally used lasers emitting at 1  $\mu\text{m}$  or 10  $\mu\text{m}$ . For defense specifically, applications include Directed Infrared Counter Measures (DIRCM), providing protection for aircraft from anti-aircraft missiles. Mid-infrared lasers may also be used as target designators and for range finding. Free space communication is also possible, provided the laser wavelength coincides with an atmospheric transmission window, as shown in Figure 1. Remote sensing of gases such as  $\text{CO}_2$  as well as remote wind speed measurements are also possible [4]. However, the need remains to improve these sources with regard to size, brightness, efficiency, and wavelength range. With the development of a wider range of lasers operating in the mid-infrared region, it is foreseen that even more applications will be identified.

One approach that has proven to be successful for generating laser light in the mid-infrared region is the use of thulium ( $\text{Tm}^{3+}$ ) and holmium ( $\text{Ho}^{3+}$ ) based solid-state lasers, where the thulium laser emitting at  $\sim 1.9$   $\mu\text{m}$  acts as pump source for the holmium laser that emits at  $\sim 2.1$   $\mu\text{m}$ . The properties of holmium, in a variety of host materials, make holmium lasers attractive pump sources for Optical Parametric Oscillators (OPO) and optically-pumped molecular lasers that in turn provide coherent light at even longer wavelengths in the mid-infrared region [5]. One thing that makes this particular scheme so attractive is that thulium lasers can be efficiently pumped with readily available laser diodes operating at 792 nm. With good efficiencies obtainable at every step of the scheme, this approach does not only have the potential to lead to efficient high-powered laser systems, but also cost-effective ones, fit for use beyond the confines of a research laboratory.

One research topic in our group was the development and experimental implementation of efficient high-power and high-energy holmium laser systems based on this pumping scheme. These 2  $\mu\text{m}$  sources could then be used as pump sources for the generation of laser light in the 3-5  $\mu\text{m}$  as well as the 8-12  $\mu\text{m}$  regions where efficient atmospheric transmission is also possible (Figure 1). This was achieved with the successful implementation of several novel laser systems, ranging from a highly efficient Ho:YLF laser and Ho:YLF MOPA system, to a single-frequency Ho:YLF ring laser amplified by a slab laser. This paper provides an overview of these systems and the scaling techniques employed.

\*wsk747@gmail.com; phone +27 12 841 3813; www.csir.co.za

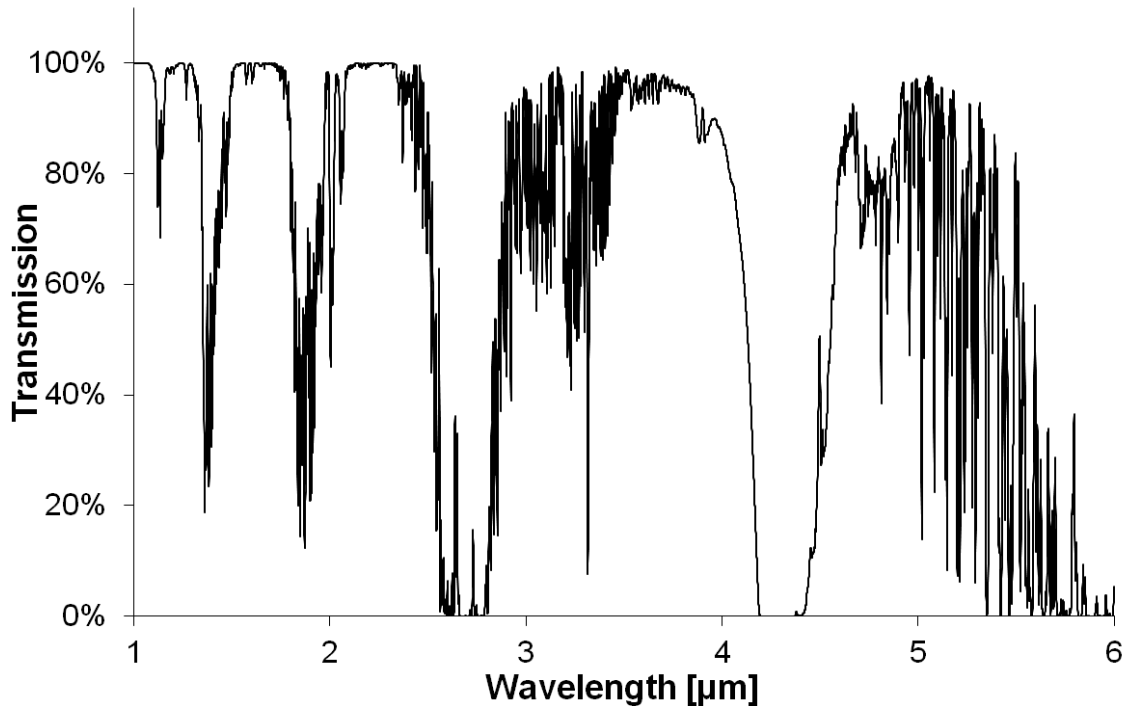


Figure 1: Atmospheric transmission of light from 1 to 6  $\mu\text{m}$ , as generated by IRTRANS4 (4.2 km propagation distance from space to ground), provides a good indication where lasers may operate for effective free space propagation [6].

## 2. THE THULIUM-HOLMIUM PUMPING SCHEME

Initial work on holmium lasers operating in the 2  $\mu\text{m}$  region involved flash-lamp pumped systems using Cr, Tm, Ho co-doped crystals [3]. In these systems  $\text{Cr}^{3+}$  absorbed light from the flash lamp into the pump energy band after which the energy could be transferred to a  $\text{Tm}^{3+}$  ion. Cross relaxation between an excited thulium ion (in level  $^3\text{H}_4$ ) and one in the ground state ( $^3\text{H}_6$ ) would then leave both the thulium ions excited in the  $^3\text{F}_4$  manifold. Energy transfer is then possible between the  $^3\text{F}_4$  state of the thulium ion to the  $^5\text{I}_7$  level of an adjacent  $\text{Ho}^{3+}$  ion, after which stimulated emission could occur to the  $^5\text{I}_8$  level, emitting a photon with a wavelength in the 2  $\mu\text{m}$  region.

This approach delivered limited efficiencies however, with pump light absorption by Cr being low as the flash lamp's emission spectrum is inherently broad when compared to the relevant absorption bands of the Cr ions. The complexity of the flash lamp high-voltage power supplies in addition to the heat load inherent to flash lamp-pumped systems did not make this design approach very desirable [7].

With high-power laser diodes becoming available, another approach to develop holmium lasers by using crystals co-doped with  $\text{Tm}^{3+}$  and  $\text{Ho}^{3+}$  became feasible [8]. Since high-power, high-brightness laser diodes emitting at 1.9  $\mu\text{m}$  are not yet readily available for directly pumping holmium, one may use thulium which can be pumped by commercially available laser diodes at  $\sim 0.8 \mu\text{m}$  as an intermediary. In this scheme a photon from the laser diode excites a thulium ion to the  $^3\text{H}_4$  level. Cross relaxation between the excited thulium ion and a thulium ion in the ground state ( $^3\text{H}_6$ ) would then leave both the thulium ions excited in the  $^3\text{F}_4$  level. Depending on the efficiency by which the Tm-Tm cross relaxation can occur, one can thus obtain two thulium ions in the excited state for one pump photon; the so-called "two-for-one" process. Energy transfer is then possible between the  $^3\text{F}_4$  state of a thulium ion to the  $^5\text{I}_7$  level of an adjacent  $\text{Ho}^{3+}$  ion, after which stimulated emission can occur to the  $^5\text{I}_8$  level, emitting a photon with a wavelength in the 2  $\mu\text{m}$  region. As there is a good spectral overlap of the laser diode and the absorption features of thulium this approach can lead to efficient pump light absorption, aiding optical-to-optical efficiency. However, due to a strong upconversion process in which energy is transferred from the excited  $^3\text{F}_4$  and  $^5\text{I}_7$  states of the thulium and holmium ions respectively, co-doped

systems have reduced upper-state lifetimes resulting in reduced energy storage efficiencies which are detrimental to pulsed laser performance. Upconversion also leads to an increase in thermal heat load in the laser crystal [9]. This can also result in an increase in thermal lensing leading to degradation in beam quality, and even thermal fracture in severe cases.

An elegant solution to prevent this fundamental problem of parasitic energy transfer processes between the thulium and holmium ions is to host these two rare-earth ions in separate crystals [10]. This approach eliminates the upconversion processes between thulium and holmium. In addition, a more modular design where a diode-pumped thulium laser module can pump a holmium laser module is made possible. This design approach and accompanying excitation scheme is depicted in Figure 2. In this case a crystal singly-doped with thulium is optically pumped with a high power laser diode at  $\sim 0.8 \mu\text{m}$ , exciting  $\text{Tm}^{3+}$  ions from the ground state to the  $^3\text{H}_4$  state. Cross relaxation between an excited thulium ion and a thulium ion in the ground state ( $^3\text{H}_6$ ) would then leave both the thulium ions excited in the  $^3\text{F}_4$  level. The thulium laser could then lase from the  $^3\text{F}_4$  level to the ground state ( $^3\text{H}_6$ ), emitting  $\sim 1.9 \mu\text{m}$  laser light. This laser light is then used to pump a laser crystal which is only doped with holmium, exciting a  $\text{Ho}^{3+}$  ion from its ground state ( $^5\text{I}_8$ ) to the upper laser level  $^5\text{I}_7$ . Stimulated emission then occurs from  $^5\text{I}_7$  back to the ground state  $^5\text{I}_8$ , emitting at  $\sim 2.05 \mu\text{m}$ .

This approach has several advantages over the first two approaches discussed in this section. The elimination of the parasitic energy transfer processes between the thulium and holmium ions in co-doped crystals leads to a decrease in heat load. The absence of these processes also increases the effective upper level lifetime of holmium, which is beneficial for efficient pulsed operation. The doping of the holmium laser crystals can now also be selected independently of that of the thulium, choosing a doping which is optimal for the desired holmium laser design; be it for continuous or pulsed operation. The Ho doping level can also be chosen sufficiently low to avoid detrimental Ho-Ho upconversion processes [12]. Finally, with most of the system heat load now residing in the thulium laser, and the small quantum defect between the holmium laser's pump and laser photons leading to a low heat load, the holmium laser will experience less heat induced optical aberrations, making near-diffraction-limited laser beams at high output powers possible.

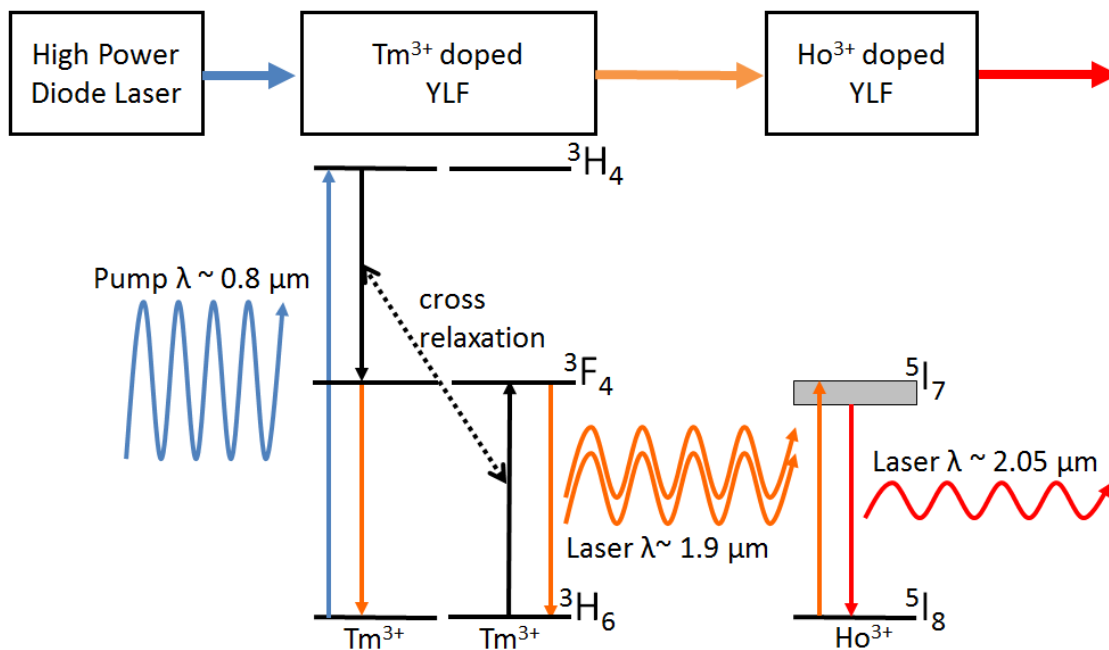


Figure 2: Pumping scheme of a laser diode-pumped Tm laser pumping a Ho laser [11].

### 3. PROPERTIES OF HO:YLF

Figure 3 shows a schematic of the Ho:YLF energy levels and transitions relevant to this work. When pumping at ~1940 nm (or 1890 nm), holmium ions in the  $^5I_8$  ground state, which absorb the pump photons, get excited to the upper laser level  $^5I_7$ . This upper laser level is meta-stable with a long lifetime of ~14 ms [13]. Holmium ions in the excited state ( $^5I_7$ ) can then decay back to the  $^5I_8$  ground state through stimulated emission. Since Ho:YLF is a birefringent crystal, a Ho:YLF laser using an a-cut crystal (where the c-axis is perpendicular the optical axis) can emit at either 2050 nm, or 2064 nm, depending on the polarization chosen in the oscillator design (blue arrows in Figure 3). Thereafter, rapid thermalisation on the picosecond scale restores the Boltzmann distribution in the ground state.

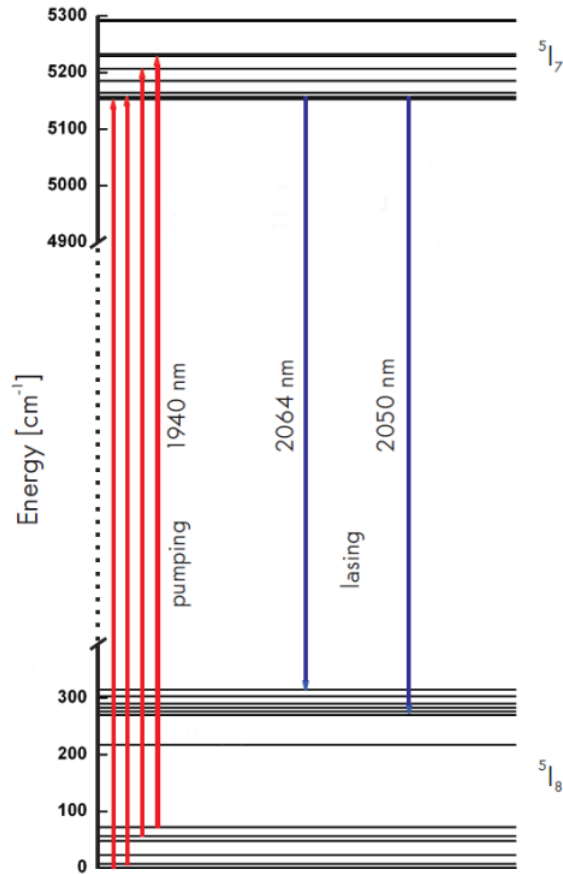


Figure 3: Scheme of the energy levels of interest for pumping Ho:YLF lasers.

Detailed analysis of Ho:YLF's spectroscopic properties has previously been done by Walsh et al. and Payne et al. ([13] & [14]). The relevant polarisation dependent absorption and emission spectra reported in [13] are shown in Figure 4. This data is for 0.5 % doped Ho:YLF crystals at a temperature of 300 K.

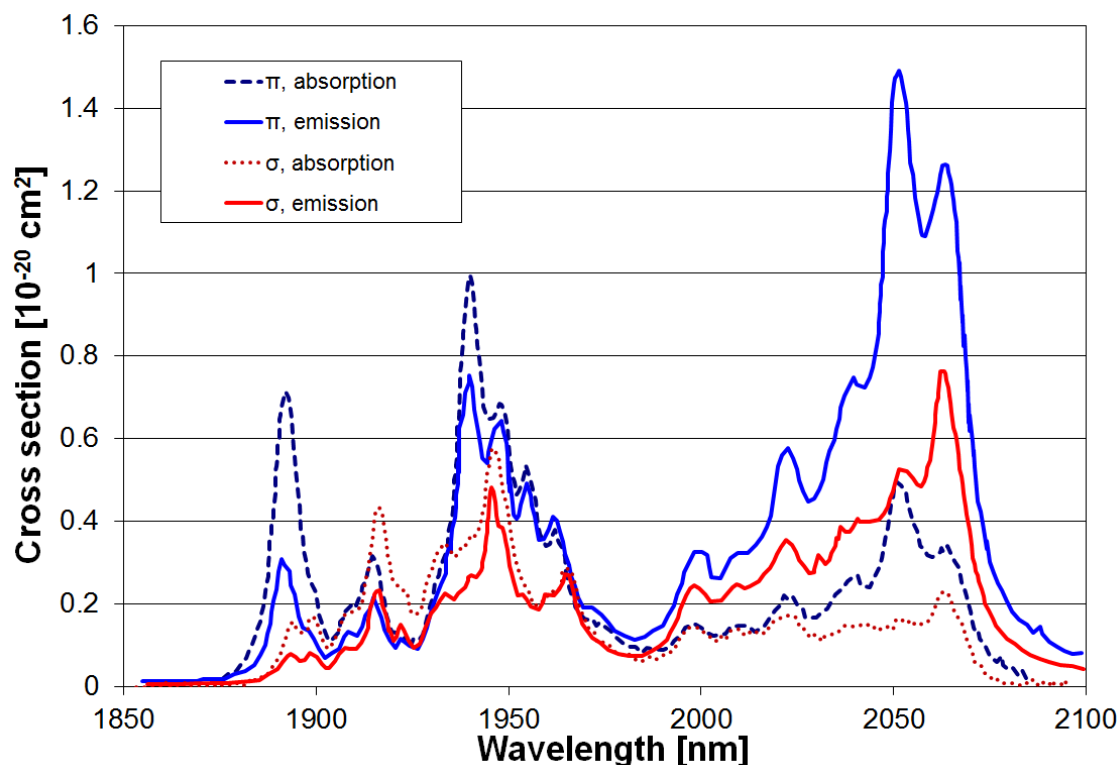


Figure 4: Absorption and emission cross sections of Ho:YLF on the  $\pi$ - and  $\sigma$ -sigma polarizations from 1850 to 2100 nm [13].

Of interest to this work is the 1.8 to 2.1  $\mu\text{m}$  region where the  $^5I_7 \leftrightarrow ^5I_8$  transition gives rise to the spectra shown in Figure 4. For pumping Ho:YLF the two absorption peaks at 1891 nm and 1940 nm are of interest. Pumping at 1891 nm is possible with Tm:YLF lasers while 1940 nm is accessible with Tm: fiber lasers, which have been commercially available for several years now from *IPG Photonics*. However the uniaxial crystal structure of Ho:YLF results in the absorption and emission cross sections being polarisation dependent, with significant differences for  $\sigma$ - and  $\pi$ -polarisations at certain wavelengths for a-cut crystals, where the c-axis is perpendicular to the optical axis. The absorption peak centered at 1891 nm has an absorption cross section of  $\sim 0.7 \times 10^{-20} \text{ cm}^2$  for the  $\pi$ -polarisation ( $\mathbf{E} \parallel \mathbf{c}$ ) while the absorption cross section for the  $\sigma$ -polarisation ( $\mathbf{E} \perp \mathbf{c}$ ) at the same wavelength is less than  $0.06 \times 10^{-20} \text{ cm}^2$ . The absorption peak centered at 1940 nm has an absorption cross section of  $\sim 0.99 \times 10^{-20} \text{ cm}^2$  for the  $\pi$ -polarisation ( $\mathbf{E} \parallel \mathbf{c}$ ) while the absorption cross section for the  $\sigma$ -polarisation ( $\mathbf{E} \perp \mathbf{c}$ ) at the same wavelength is  $\sim 0.46 \times 10^{-20} \text{ cm}^2$ . This large difference between the two polarisations for the given wavelengths is of great importance when it comes to designing an efficient pump system for Ho:YLF as one would either have to pump with a linearly polarised laser, or implement a polarisation-based pumping scheme to ensure good absorption.

In 2005 Dergachev et al. used an unpolarized Tm: fiber laser manufactured by *IPG photonics* to end-pump a two crystal Ho:YLF laser [15]. The Tm: fiber laser delivered 100 W of unpolarized laser light at 1940 nm. The fiber laser's wavelength was selected to coincide with the strong  $\pi$ -polarization absorption peak of Ho:YLF. But, as absorption in Ho:YLF at 1940 nm is strongly polarization dependent, pumping a single a-cut crystal with unpolarized light would result in inefficient pump light absorption. This was addressed by splitting the unpolarized pump light from the fiber laser into two polarized beams using a polarizing beam splitter (PBS) and then pumping two Ho:YLF crystals placed in the same resonator separately. This design approach proved effective, with the holmium laser producing up to 43 W of cw output and 45 mJ per pulse in the Q-switched regime.

The approach of splitting the unpolarized laser light from Tm: fiber lasers into vertically and horizontally polarized beams to pump separate Ho:YLF crystals was not limited to single oscillators containing two crystals. This approach

could also be applied to Master Oscillator Power Amplifier (MOPA) systems, as subsequently demonstrated by Dergachev et al. in 2007 [16]. For this system a 120 W Tm: fiber laser, manufactured by *IPG Photonics*, was used to pump an oscillator and amplifier crystal by once again splitting the unpolarized pump beam into two linearly polarized beams in order to pump the two crystals separately. In addition to efficiently using an unpolarized pump source to pump birefringent crystals, the MOPA configuration was a good approach for energy scaling, decreasing the intra-cavity fluence in the oscillator when compared to the case where one would have the two crystals in a single laser cavity. This MOPA delivered up to 55 mJ at a PRF of 500 Hz when Q-switched, and 42 W of average power in cw mode.

Subsequently, Dergachev et al. extended this pumping scheme to two-crystal Ho:YLF amplifiers [17]. A single 120 W unpolarized Tm: fiber laser pumped two Ho:YLF amplifier crystals separately. The seed beam passed through both crystals once. Two of these amplifiers were used in series to amplify the output of a Ho:YLF MOPA similar to the one described in [16]. This cascaded amplifier scheme delivered up to 115 W cw output, and 170 mJ per pulse at 100 Hz when the seed laser was Q-switched.

While Dergachev et al. split the unpolarized light into two linear polarized beams in order to efficiently pump two Ho:YLF crystals separately, Bai et al. used two crystals of different doping (0.5 and 1.0 %) pumped collinearly with a single unpolarized Tm: fiber laser [18]. Although this improved the effective absorption of the pump light, overall efficiency was relatively low, possibly hampered by the increased parasitic processes related to the higher doping in the second crystal. In other work, single crystal designs were also implemented, leading to decreased optical-to-optical efficiency, but with the advantage of a more simple design which did not require any polarization-dependent optics for the unpolarized pump light [19], [20].

#### 4. A COMPACT HO:YLF MOPA

In 2010 our group reported that it was possible to efficiently utilize the unpolarized pump light from a thulium fiber laser to pump Ho:YLF crystals [12]. This was possible by placing two a-cut Ho:YLF crystals with their c-axes perpendicular to each other and pumping them collinearly with the unpolarized pump beam, as shown in Figure 5.

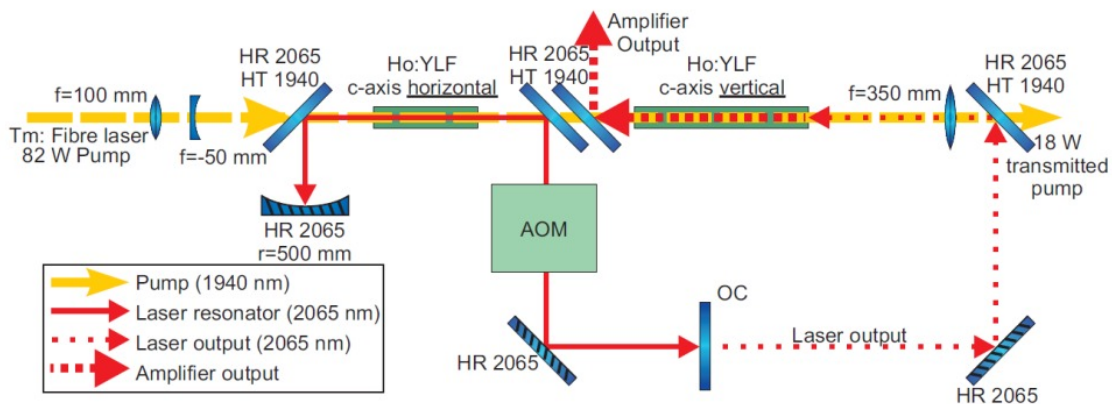


Figure 5: A schematic of the Ho:YLF MOPA system. The system utilized the unpolarized beam from a Tm: fiber laser to pump two Ho:YLF crystals in series [12].

The first crystal resided in the oscillator while the second was used as an amplifier crystal. The first crystal was orientated with its c-axis horizontal and, because the crystal absorbed pump light predominantly on its  $\pi$ -polarization, it absorbed mostly horizontally polarized light. The remaining pump light transmitted through the first crystal was therefore partially vertically polarized. To maximize absorption of this partially polarized pump light, the second crystal was placed with its c-axis orientated vertically. With the oscillator forced to operate vertically polarized by the use of a polarization-dependent 45 degree mirror (HRs & HTp at 2065 nm), the linearly polarized seed light entering the amplifier crystal was amplified on the  $\pi$ -polarization. This specific combination of crystal orientations and laser light polarization had the advantage that the laser operated on the  $\sigma$ -polarization of the first crystal, whose weak thermal

lensing enabled near diffraction-limited beam quality, while the second crystal provided high gain on the  $\pi$ -polarization which had the higher emission cross-section. Pumping these two crystals in series with the same pump also minimized the pump propagation distance which decreased atmospheric absorption of the pump light which could lead to detrimental effects such as thermal blooming [21].

With the oscillator emitting up to 12.4 W cw at 2065 nm, the single-pass amplifier provided a gain of nearly 2, emitting up to 23.7 W when in continuous wave mode. When pulsed, the MOPA system delivered up to 21.3 mJ at a PRF of 1 kHz (Figure 6). These experimental results compared well with simulation work done by Martin Schellhorn [12]. One of the outcomes of this work was the conclusion that parasitic upconversion processes are negligible for 0.5 % doped Ho:YLF crystals.

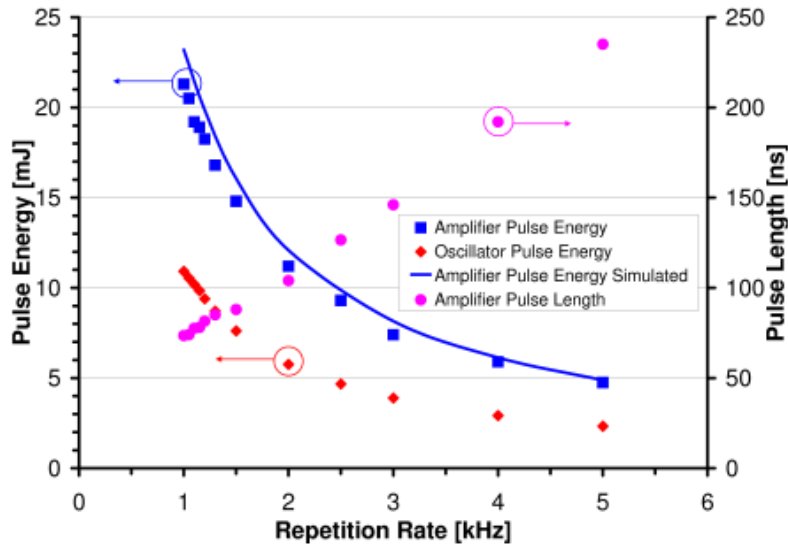


Figure 6: The oscillator and amplifier output energy as a function of pulse repetition frequency (left axis) as well as the pulse length (right axis)

## 5. A SINGLE-FREQUENCY HO:YLF RING LASER

As the work reported in [12] showed the collinear crystal pump design to be an elegant and efficient way to utilize unpolarized pump light, an injection-seeded, single-frequency Ho:YLF ring-laser with single-pass amplifier was subsequently developed by our group, using this pumping scheme. A schematic of the system is shown in Figure 7. The laser was locked to the P(9) absorption line of HBr at 2064.12 nm; seeded with a single-frequency diode laser. A total of three crystals were pumped in series by the same thulium fiber laser that was previously used in [12]. The oscillator contained a single a-cut Ho:YLF crystal while the amplifier consisted of two a-cut holmium YLF crystals. While up to 18 W of pump light could be transmitted through the crystals in [12], pump light absorption on the first pass in this ring laser and amplifier was good enough that the total remaining pump power left was sufficiently low for it to be back-reflected into the crystals for a second pass (without feedback to the fiber laser), thereby improving overall performance. Although this system effectively absorbed all of the available pump light, its optical-to-optical efficiency was relatively low as a larger pump beam size and resonator mode was necessary in order to prevent optical damage at the low repetition rates this system was designed to operate at (PRF from 1 to 350 Hz).

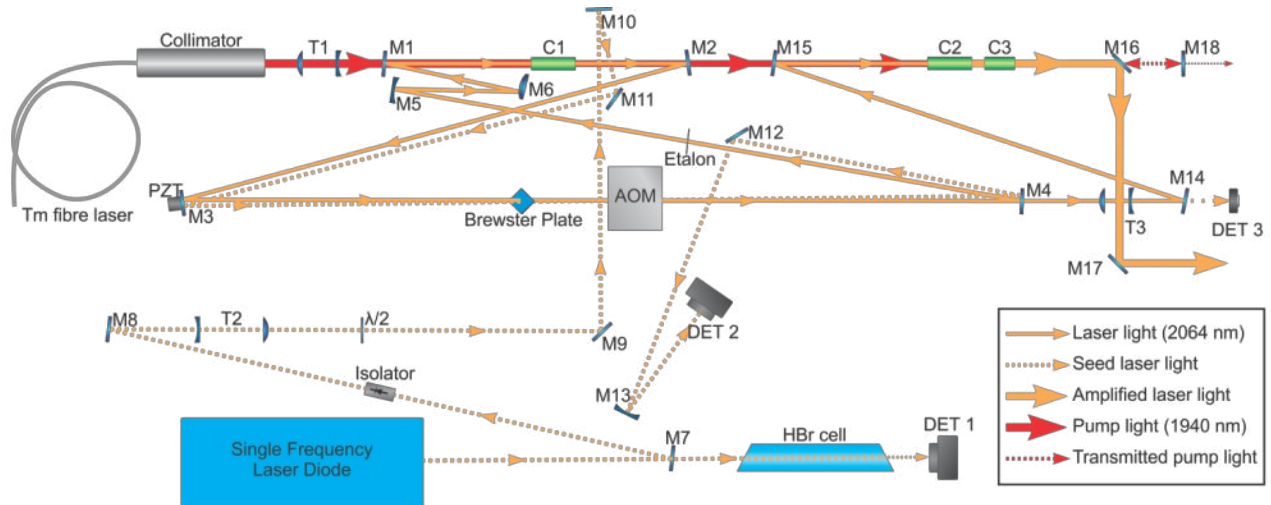


Figure 7: The single-frequency Ho:YLF ring laser and single-pass amplifier developed subsequent to [12]. The MOPA system also used the full unpolarized beam from the same Tm: fiber laser to pump multiple Ho:YLF crystals whose c-axes were orientated perpendicular with regard to each other [22].

The system delivered up to 72 mJ of energy per pulse at a pulse repetition frequency (PRF) of 50 Hz in a near-diffraction limited beam ( $M^2 < 1.1$ ) at 2064 nm. The laser's full width at half maximum (FWHM) pulse length varied with PRF from ~320 ns at 10 Hz to 600 ns at 350 Hz.

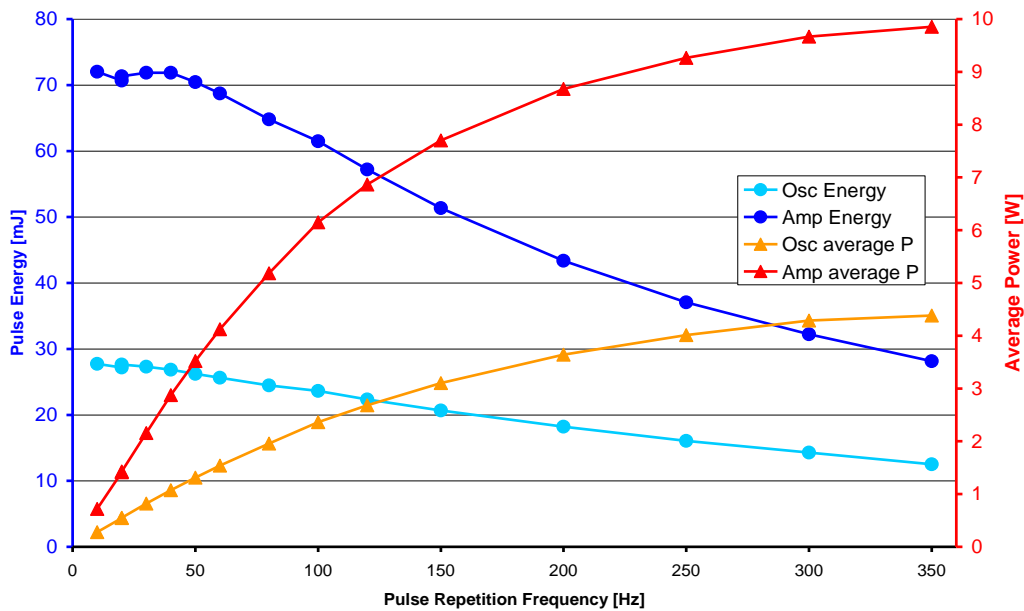


Figure 8: Output energy of the ring laser and amplifier at different pulse repetition frequencies (left). The average output power at different repetition rates are indicated on the right axis.



## 6. A Tm:YLF SLAB LASER TO PUMP A HO:YLF AMPLIFIER

The Ho:YLF laser and amplifier systems described in Sections 3 to 5 were pumped by commercially sourced 1.9  $\mu\text{m}$  Tm: fiber lasers. Unfortunately these commercial lasers are currently limited to a maximum of 120 W of cw output power for the water-cooled systems and 50 W per laser for the air-cooled models [23]. Scaling Ho:YLF output to higher powers and/or energies would require several of these lasers, as demonstrated in [17] where three 120 W water-cooled systems were used. While these fiber lasers exhibit several desirable properties such as excellent beam quality ( $M^2 < 1.1$ ), stability and compactness, as well as acceptable wall plug efficiencies; this approach can prove to be quite a costly exercise as there is currently a limited number of suppliers capable of supplying reliable Tm: fiber laser systems at these power levels.

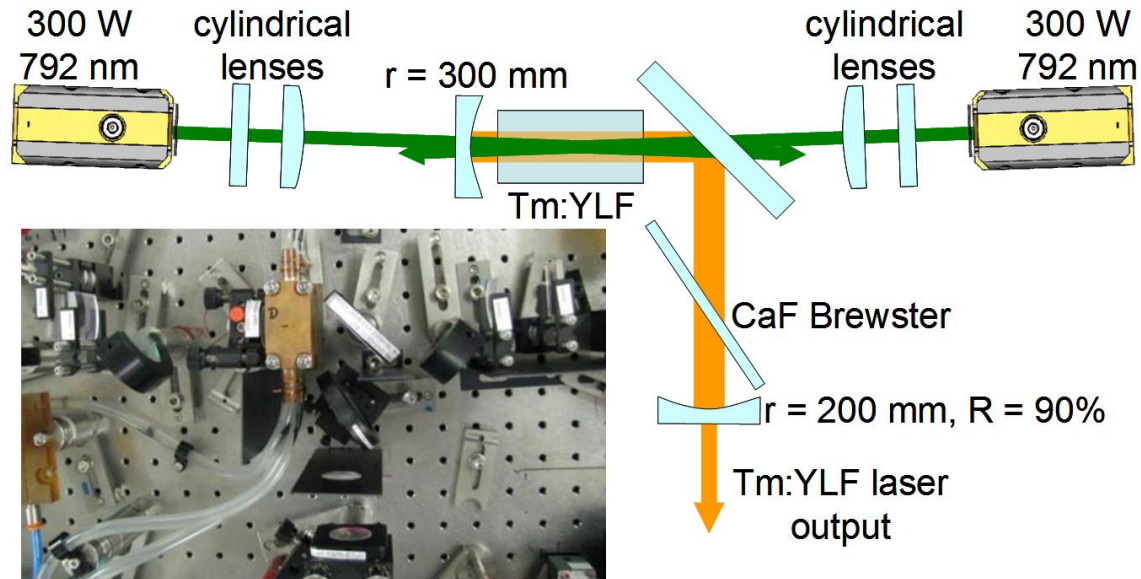


Figure 9: Schematic of the Tm:YLF slab laser. A top-view photo of the laser layout is shown in the insert, bottom left [27].

An attractive alternative for generating 1.9  $\mu\text{m}$  laser light to pump holmium-doped systems with, are Tm:YLF lasers. These lasers had limited output powers though, held back by the low thermal fracture limit of the host material. YLF does have several beneficial properties, however, such as low thermal lensing, and a natural birefringence which can aid laser design. Fortunately successful power scaling was demonstrated collaboratively using an end-pumped slab laser geometry, delivering up to 148 W of laser power at 1912 nm from a Tm:YLF slab laser [24]. This was a significant improvement over the previous record power of 68 W from a Tm slab laser [25]. The laser slab geometry proved a particularly successful power scaling strategy for Tm:YLF as it allowed for efficient cooling from both the top and bottom of the crystal. Additionally the elongated shape of the crystal is well suited for end-pumping by laser diode stacks whose beams are usually highly astigmatic.

Subsequently we developed a Tm:YLF slab laser with the aim of using it to pump Ho:YLF crystals [26]. It consisted of an a-cut Tm:YLF crystal (with its c-axis horizontally orientated, orthogonal to the optical axis of the laser) end-pumped pumped by two 300 W laser diode stacks emitting at 792 nm. The highest output power of 225 W was obtained at an output wavelength of 1909 nm, with the laser operating on the  $\sigma$ -polarization of the crystal. This wavelength, however, is undesirable for use with Ho:YLF as its absorption cross section is less than  $0.2 \times 10^{-20} \text{ cm}^2$  at 1909 nm, as indicated in Figure 4. This would result in low absorption of the pump light in the planned Ho:YLF amplifier with which we wanted to amplify the ring laser's output with. We thus redesigned the laser to operate on  $\pi$ , emitting laser light in the region of 1890 nm instead. This was done by insertion of a  $\text{CaF}_2$  Brewster plate which would induce loss for the  $\sigma$ -polarization, but not for the  $\pi$ -polarization. With the absorption cross section of Ho:YLF being  $\sim 0.6 \times 10^{-20} \text{ cm}^2$  at 1890 nm (for  $\pi$ -polarization), far better absorption would be obtained in the planned Ho:YLF amplifier system [13].

The resulting wavelength was measured to be in the region of 1890 nm for all output powers. A maximum output power of 189 W was obtained from the laser with a slope efficiency of 38 % with regard to incident pump power and an optical-to-optical efficiency of 34 %. At full power, the beam quality factor ( $M^2$ ) was measured to be 3.8 in the vertical axis and 440 in the horizontal. The Tm:YLF slab laser was subsequently used in this configuration to pump the Ho:YLF amplifier, as discussed in the subsequent section.

### 7. DOUBLE-PASS HO:YLF SLAB AMPLIFIER

We previously demonstrated 210 mJ single-frequency 2  $\mu$ m pulses by using a two-crystal Ho:YLF & Ho:LuLF single-pass slab amplifier [28]. Subsequent simulations based on a space-resolved rate-equation model indicated that using longer gain crystals and double passing the seed beam would lead to a significant increase in gain and thus greater output energies [29]. Based on the simulation results we subsequently used two 0.5 % at. doped Ho:YLF crystal slabs in series. Both crystals were 10 mm wide, 2 mm thick and 50 mm long and were a-cut with their c-axes horizontal. The experimental setup is illustrated in Figure 10. The slabs were placed in series to provide a total of 200 mm in gain length when double passed.

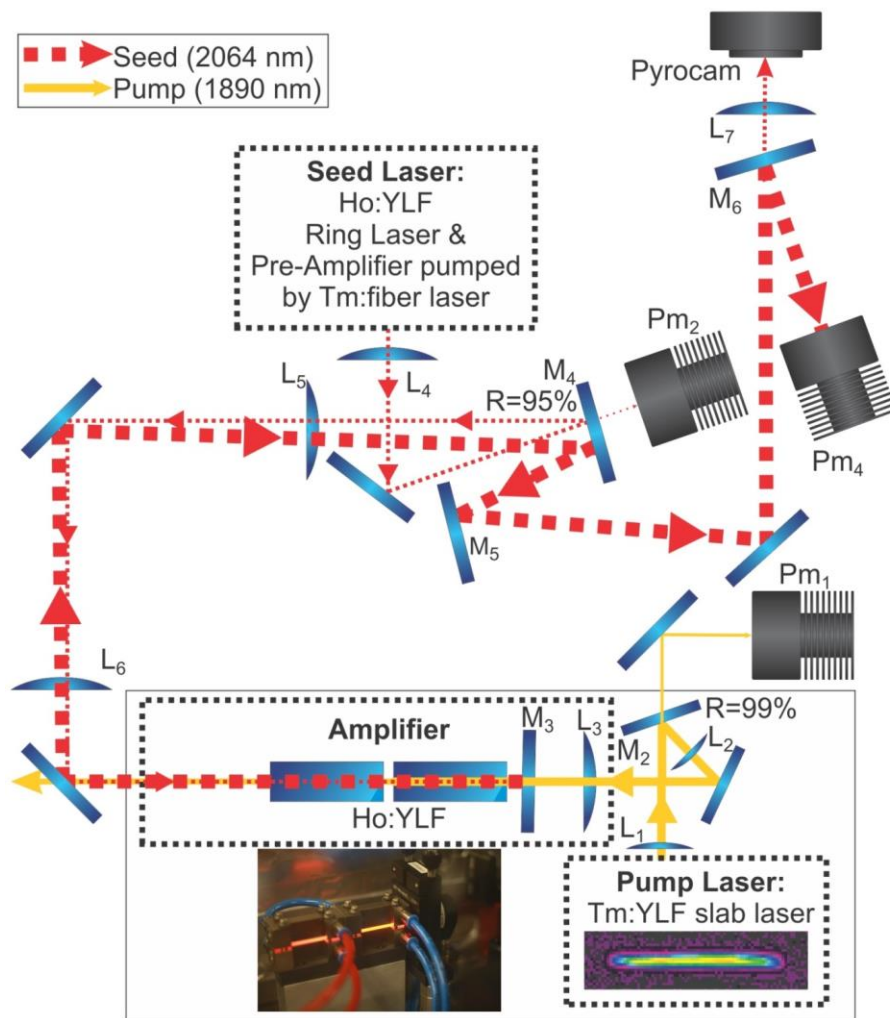


Figure 10: Schematic of the experimental setup for the double-pass Ho:YLF slab amplifier. A photo of the mounted slab crystals is shown in the insert [30].

As pump source we used the Tm:YLF slab laser described in the previous section. The incident pump light's polarization was horizontal so that the pump light was absorbed by the stronger absorbing  $\pi$ -polarization of the Ho:YLF crystals. The seed laser for the amplifier was the injection-seeded, single-frequency Ho:YLF ring-laser with pre-amplifier, as described in Section 5. The seed polarization was kept vertical (perpendicular to the crystal c-axis) so that the seed beam was amplified on the  $\sigma$ -polarization of the Ho:YLF slabs, which has an intrinsic weak thermal lens, at the cost of lower gain due to its lower emission cross section when compared to the  $\pi$ -polarization. Optical feedback into the master ring oscillator was prevented by inserting an optical isolator between the oscillator and its pre-amplifier. This reduced the available seed energy incident on the amplifier to  $\sim 50$  mJ at 50 Hz. The round seed beam from the ring laser was shaped to match the astigmatic gain profile of the amplifier by using cylindrical lenses. As the amplified beam passed through these same lenses on the backward path, after being reflected by  $M_3$ , the amplified beam exiting the system was roughly, circularly symmetric once more.

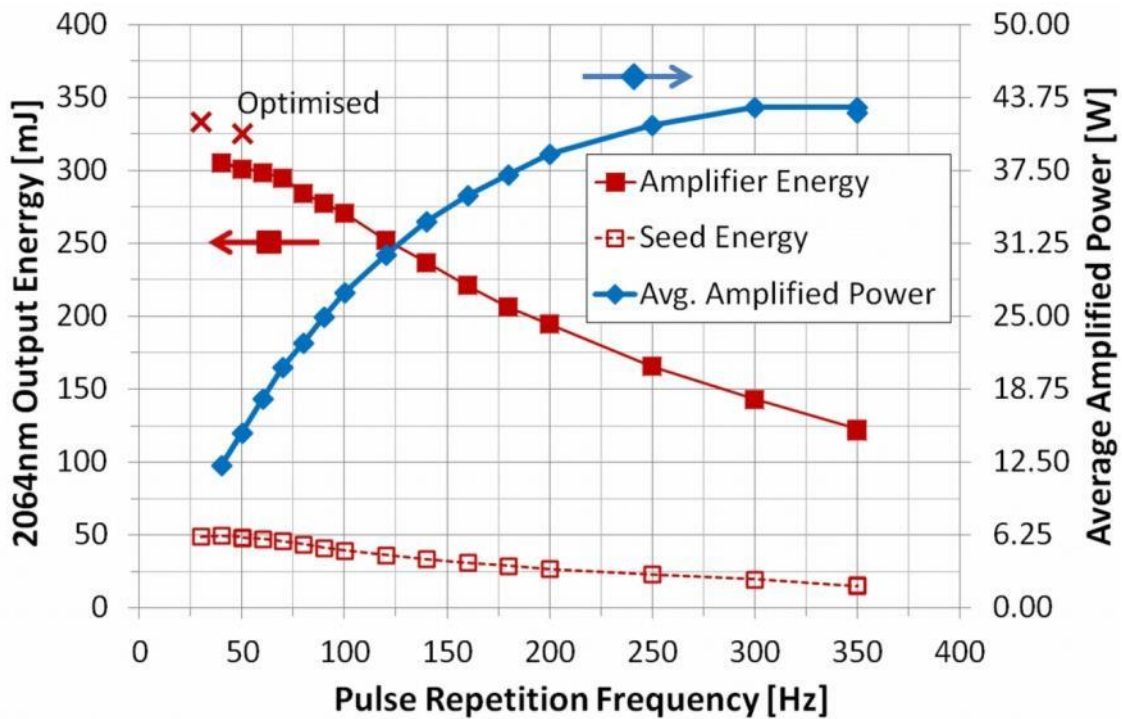


Figure 11: Seed and Amplified 2064 nm output energy (left axis) and the average power of the amplified pulses (right axis) as functions of Pulse Repetition Frequency.

A maximum pulse energy of 333 mJ was obtained from the amplifier at the lowest measured PRF of 30 Hz (Figure 11). The horizontal beam quality factor ( $M_x^2$ ) was 1.5 while the vertical ( $M_y^2$ ) was less than 1.1. This work shows that Ho:YLF amplifiers pumped with Tm:YLF slabs provide an effective way to obtain high energies at 2  $\mu\text{m}$  which could be scaled even further using the same architecture. The 2064 nm output from this amplifier was subsequently used to pump molecular HBr lasers and amplifiers [31], [32].

## 8. EFFICIENT HIGH-POWER HO:YLF LASER

Ho:YAG based solid-state lasers pumped with thulium-doped fiber lasers has been a popular approach for several years for generating coherent light at 2  $\mu\text{m}$ , delivering high average powers and good optical-to-optical efficiencies [33]. Ho:YLF was used for low pulse repetition frequency Q-switched applications due to its long upper state lifetime [16], but had more limited use in high average power applications as the low thermal fracture limit of YLF could pose a problem when pumping at the high intensity levels required for efficient cw operation. If thermal damage of Ho:YLF crystals is avoided however, efficient high-power end-pumped laser configurations can be implemented. This is possible with Tm: fiber laser pumped Ho:YLF systems as the quantum defect is particularly low, with the pump wavelength being 1940 nm and laser output at 2064 nm.

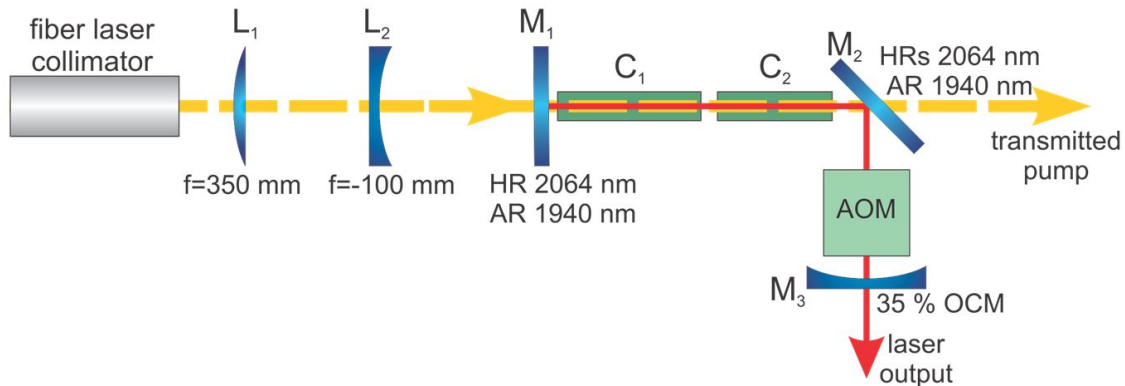


Figure 12: Experimental set-up of the Ho:YLF laser. A Tm-fiber laser pumps two collinear crystals residing in a single cavity [34].

To investigate whether the implementation of high-power Ho:YLF lasers with high-efficiencies is possible, we designed a laser with a small pump beam and corresponding mode size, pumped with a high-power thulium fiber laser. A schematic of the Ho:YLF laser layout is shown in Figure 12. As pump source, a commercial Tm-doped fiber laser was used, delivering up to 84.7 W of power in a single mode fiber at 1940 nm. The average beam radius of the pump beam in the crystals was approximately 310  $\mu\text{m}$ , almost half the size previously used in [12]. Two 0.5 % doped Ho:YLF rods were used in the cavity. The relatively low doping alleviated upconversion, but resulted in a longer gain medium being needed for sufficient absorption of the pump light. Consequently two crystals were used with lengths of 50 mm ( $C_1$ ) and 40 mm ( $C_2$ ).

The cavity consisted of an input coupler mirror ( $M_1$ ), a folding mirror ( $M_2$ ) and an output coupler mirror ( $M_3$ ). The flat 45° folding mirror ( $M_2$ ) was coated to be highly reflective at 2064 nm for the s-polarization while being highly-transmissive for the pump light (1940 nm), forcing the laser to operate on the vertical polarization. For Q-switching, an AOM was inserted between  $M_2$  and  $M_3$ . The first crystal was placed with its c-axis vertical, with the second crystal's c-axis horizontal, as illustrated in Figure 13. The polarization dependent folding mirror  $M_2$  (Figure 12) forced the laser to lase vertically polarized, extracting gain on the  $\pi$ -polarization of the first crystal, and on the  $\sigma$ -polarization of the second crystal. As the first crystal's absorption would have partially polarized the pump light of  $C_2$  due to the polarization-dependent absorption at 1940 nm in Ho:YLF,  $C_2$  mostly absorbed horizontally polarized pump light on its  $\pi$ -polarization.

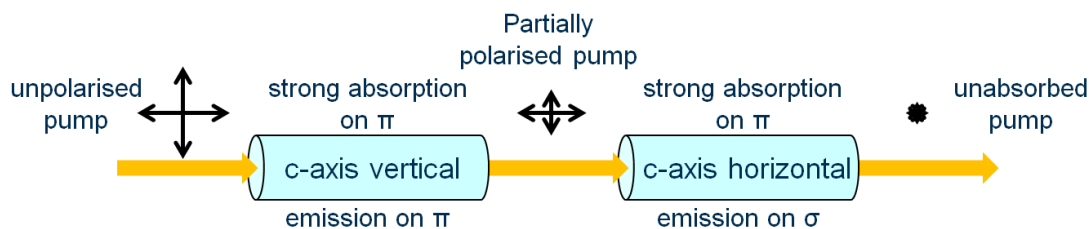


Figure 13: Two Ho:YLF crystals inside the same cavity, their c-axes rotated 90° with regard to each other in order to increase the total amount of pump light being absorbed.

The laser delivered a maximum of 45.1 W with an optical-to-optical efficiency of 53 % near room temperature, when pumped with 84.7 W. The output and efficiency compared favorably with similar Ho:YAG lasers reported upon in [33] and [35] which had optical-to-optical efficiencies of 51.3 - 60 % and 65 % respectively. The laser operated in both continuous and Q-switched modes with a near diffraction-limited beam at full power, demonstrating that Ho:YLF based lasers can deliver high average powers and optical-to-optical efficiencies simultaneously. Pulsing at a repetition frequency of 50 kHz, laser pulse durations between 46.2 and 49.2 ns long were measured. The laser's  $M^2$  was measured to be better than 1.06 at full pump power. The laser wavelength was measured to be 2063 nm.

## 9. AN EFFICIENT AND COMPACT 60 W HO:YLF MOPA

More recently, we developed a compact Ho:YLF oscillator–amplifier system end-pumped by two 54 W unpolarized Tm: fiber lasers, and produced 60.2 W of output power at 2064 nm (Figure 14, [36]).

The oscillator consisted of a flat input coupler mirror, a 50 mm long 0.5 % doped Ho:YLF crystal rod, a 45 degree folding mirror, an AOM, and a concave output coupler mirror. The oscillator operated vertically polarized on the holmium crystal's  $\sigma$ -polarization, ensuring good beam quality from the weak thermal lens. The concave output coupler had a radius of 300 mm and a reflectivity of 82 % at 2064 nm. The oscillator gave a maximum output of 24 W with an  $M^2$  of 1.06.

The single-pass amplifier consisted of two 40 mm long, 0.5 % doped, Ho:YLF crystal rods and four folding mirrors. While the seed laser was pumped by a single fiber laser, the amplifier utilized the transmitted pump light from the seed laser in addition to the second fiber laser. With the first crystal amplifying on the  $\sigma$ -polarization and the second crystal on the  $\pi$ -polarization, the amplifier delivered 60.2 W with an  $M^2$  of 1.09, representing a gain of 2.5 while achieving an optical-to-optical efficiency of 55.5 %. When Q-switched with the AOM, the system delivered pulse lengths of between 43 and 113 ns at repetition rates from 15 to 40 kHz, as indicated in Figure 15. This MOPA system was semi-ruggedized, and was subsequently used to pump optical parametric oscillators emitting in the 3-5  $\mu\text{m}$  and the 8  $\mu\text{m}$  region.

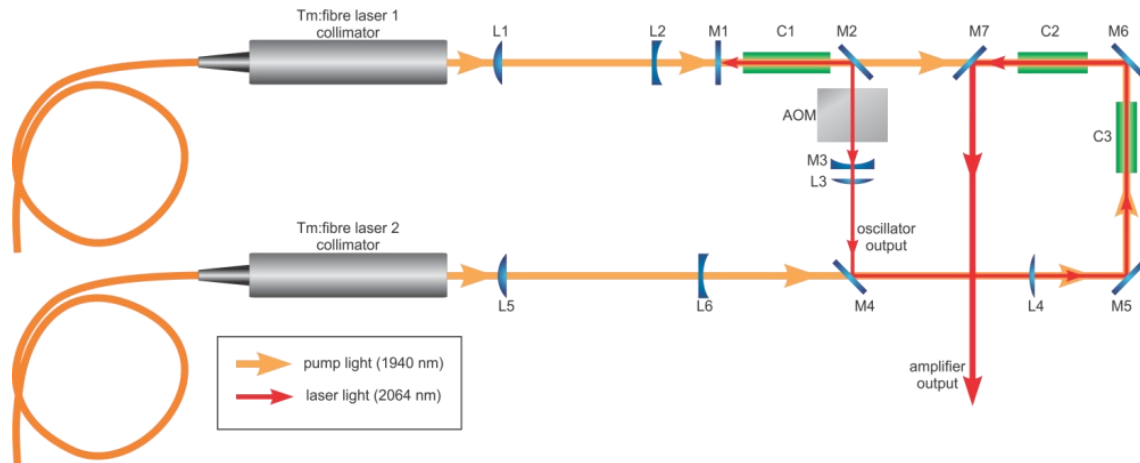


Figure 14: Schematic diagram of the Ho:YLF Master Oscillator Power Amplifier system [36].

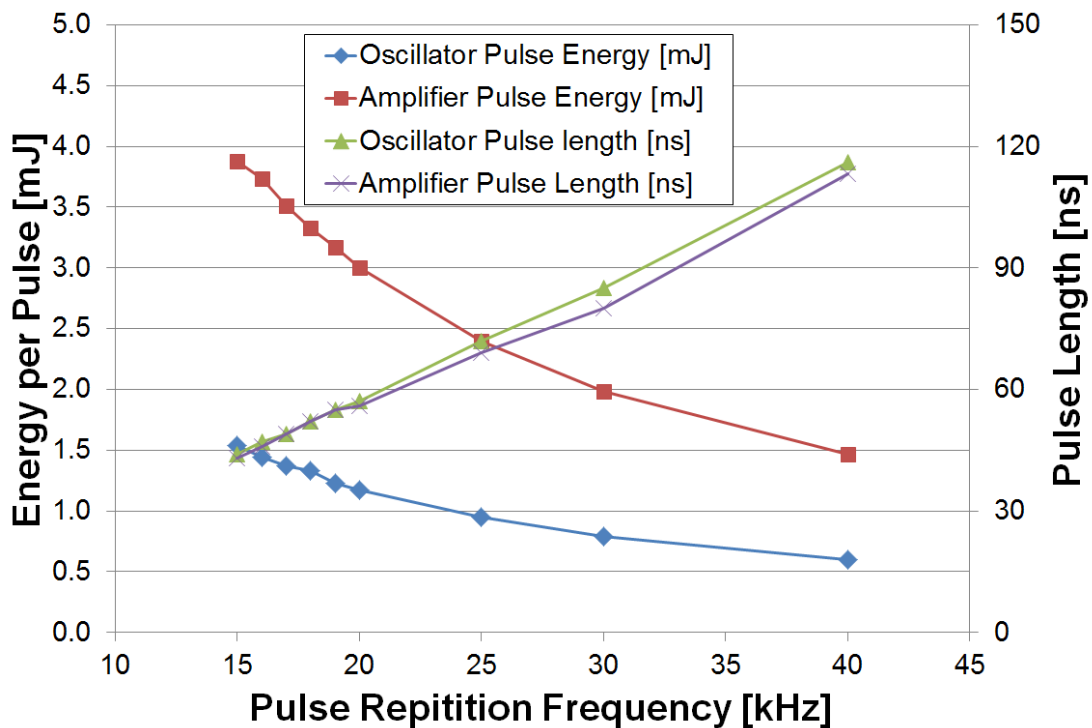


Figure 15: Oscillator and amplifier output energy (left axis) and FWHM pulse lengths (right axis) of the 60 W Ho:YLF MOPA as a function of the pulse repetition rate at full pump power.

## 10. CONCLUSION

With the use of thulium and holmium doped YLF, a diverse range of 2  $\mu\text{m}$  lasers and amplifiers were developed which varied from high-energy, single-frequency oscillators and amplifiers, to compact and efficient Ho:YLF MOPA systems delivering high average powers. This was made possible by exploiting various advantageous properties of holmium-doped YLF while mitigating its detrimental properties through the use of novel pump and laser design approaches. The pumping and scaling techniques that have been illustrated could be used in other bulk birefringent quasi 3-level laser materials to improve output powers and energies, as well as optical-to-optical efficiencies.

## REFERENCES

- [1] L. Johnson, G. Boyd, and K. Nassau, "Optical maser characteristics of Tm<sup>3+</sup> in CaWO<sub>4</sub>," *Proc. IRE*, vol. 50, no. 86, 1962.
- [2] L. Johnson, G. Boyd, and K. Nassau, "Optical maser characteristics of Ho<sup>3+</sup> in CaWO<sub>4</sub>," *Proc. IRE*, vol. 50, no. 87, 1962.
- [3] I. T. Sorokina and K. L. Vodopyanov, *Solid-state mid-infrared laser sources*, vol. 89. Springer Science & Business Media, 2003.
- [4] F. Gibert, D. Edouart, C. Cénac, and F. Le Mounier, "2 micron high-power multiple-frequency single-mode Q-switched Ho: YLF laser for DIAL application," *Applied Physics B*, vol. 116, pp. 967–976, 2014.
- [5] E. Lippert, "Progress with OPO-based systems for mid-IR generation," in *SPIE Security+ Defence*, 2011, p. 81870F–81870F.
- [6] UKIRT, "This data, produced using the program IRTRANS4, was obtained from the UKIRT worldwide web pages," 2013. [Online]. Available: <http://www.jach.hawaii.edu/UKIRT/astronomy/utls/atmos-index.html>. [Accessed: 2013]
- [7] E. P. Chicklis, C. S. Naiman, D. R. Folweiler, D. R. Gabbe, H. P. Jenksen, and A. Liz, "High-Efficiency Room Temperature 2.06 micron Laser using sensitized Ho:YLF," *Applied Physics Letters*, vol. 19, no. 119, 1971.
- [8] T. Y. Fan, G. Huber, R. L. Byer, and P. Mitzscherlich, "Spectroscopy and diode laser-pumped operation of Tm,Ho:YAG," *IEEE Journal of Quantum Electronics*, vol. 24, no. 6, pp. 924–933, 1988.
- [9] G. Rustad and K. Stenersen, "Modeling of laser-pumped Tm and Ho lasers accounting for upconversion and ground-state depletion," *Quantum Electronics, IEEE Journal of*, vol. 32, no. 9, pp. 1645–1656, 1996.
- [10] R. Hayward, W. Clarkson, and D. Hanna, "High-power room-temperature intracavity-pumped Ho: YAG laser," in *Lasers and Electro-Optics Europe, 2000. Conference Digest. 2000 Conference on*, 2000, p. 1–pp.
- [11] W. Koen, H. J. Strauss, C. Bollig, and M. J. D. Esser, "High-power diode-end-pumped Tm:YLF slab laser delivering 189 W at," in *The 55th Annual Conference of the South African Institute of Physics*, 2010, p. 205.
- [12] W. Koen, C. Bollig, H. Strauss, M. Schellhorn, C. Jacobs, and M. Esser, "Compact fibre-laser-pumped Ho: YLF oscillator-amplifier system," *Applied Physics B*, vol. 99, no. 1, pp. 101–106, 2010.
- [13] B. M. Walsh, N. P. Barnes, and B. Di Bartolo, "Branching ratios, cross sections, and radiative lifetimes of rare earth ions in solids: application to Tm<sup>3+</sup> and Ho<sup>3+</sup> ions in LiYF<sub>4</sub>," *Journal of applied physics*, vol. 83, no. 5, pp. 2772–2787, 1998.
- [14] S. A. Payne, L. Chase, L. K. Smith, W. L. Kway, and W. F. Krupke, "Infrared cross-section measurements for crystals doped with Er<sup>3+</sup>, Tm<sup>3+</sup>, and Ho<sup>3+</sup>," *Quantum Electronics, IEEE Journal of*, vol. 28, no. 11, pp. 2619–2630, 1992.
- [15] A. Dergachev, P. F. Moulton, and T. E. Drake, "High-power, high-energy Ho: YLF laser pumped with Tm: fiber laser," in *Advanced Solid-State Photonics*, 2005, p. 608.
- [16] A. Dergachev, D. Armstrong, A. Smith, T. Drake, and M. Dubois, "3.4 micron ZGP RISTRA nanosecond optical parametric oscillator pumped by a 2.05 micron Ho: YLF MOPA system," *Optics express*, vol. 15, no. 22, pp. 14404–14413, 2007.
- [17] A. Dergachev, D. Armstrong, A. Smith, T. Drake, and M. Dubois, "High-power, high-energy ZGP OPA pumped by a 2.05 micron Ho: YLF MOPA system," in *Lasers and Applications in Science and Engineering*, 2008, pp. 687507–687507.
- [18] Y. Bai, J. Yu, M. Petros, P. Petzar, B. Trieu, H. Lee, and U. Singh, "High Repetition Rate and Frequency Stabilized Ho:YLF Laser for CO<sub>2</sub> Differential Absorption Lidar," in *Advanced Solid-State Photonics*, 2009, p. WB22.
- [19] M. Schellhorn, "A comparison of resonantly pumped Ho: YLF and Ho: LLF lasers in CW and Q-switched operation," in *Advanced Solid-State Photonics*, 2011, p. AWA8.
- [20] Y. Bai, J. Yu, S. Chen, M. Petros, P. Petzar, and U. N. Singh, "Tm: Fiber Laser Resonantly-Pumped Ho: YLF Laser for air/space borne lidar application," in *Fiber Laser Applications*, 2011, p. FWC3.
- [21] W. S. Koen, "End-pumped solid-state lasers," 2010.
- [22] C. Bollig, M. Esser, C. Jacobs, W. Koen, D. Preussler, K. Nyangaza, and M. Schellhorn, "70 mJ Single-Frequency Q Switched Ho: YLF Ring Laser-Amplifier System Pumped by a Single 82-W Tm Fibre Laser," *Middle-Infrared Coherent Sources, Trouville, France*, pp. 8–12, 2009.
- [23] IPG, "Thulium Fiber Laser Specifications," 2015. [Online]. Available: [http://www.ipgphotonics.com/products\\_tlm\\_flm.htm](http://www.ipgphotonics.com/products_tlm_flm.htm). [Accessed: 2015]

- [24] M. Schellhorn, S. Ngcobo, and C. Bollig, "High-power diode-pumped Tm: YLF slab laser," *Applied Physics B*, vol. 94, no. 2, pp. 195–198, 2009.
- [25] S. So, J. Mackenzie, D. Shepherd, W. Clarkson, J. Betterton, and E. Gorton, "A power-scaling strategy for longitudinally diode-pumped Tm: YLF lasers," *Applied Physics B*, vol. 84, no. 3, pp. 389–393, 2006.
- [26] M. Esser, "Mid-infrared diode-pumped solid-state lasers," 2010.
- [27] W. Koen, H. J. Strauss, C. Bollig, and M. J. D. Esser, "High-power diode-end-pumped Tm:YLF slab laser delivering 189 W at 1890 nm," in *SAIP Annual Conference*, 2010, p. 205.
- [28] H. Strauss, W. Koen, C. Bollig, M. Esser, C. Jacobs, O. Collett, and D. Preussler, "Ho: YLF & Ho: LuLF slab amplifier system delivering 200 mJ, 2 micron single-frequency pulses," *Optics express*, vol. 19, no. 15, pp. 13974–13979, 2011.
- [29] O. J. P. Collett, "Modelling of end-pumped Ho:YLF amplifiers," 2013.
- [30] H. Strauss, D. Preussler, M. Esser, W. Koen, C. Jacobs, O. Collett, and C. Bollig, "330 mJ single-frequency Ho: YLF slab amplifier," *Optics letters*, vol. 38, no. 7, pp. 1022–1024, 2013.
- [31] W. Koen, C. Jacobs, C. Bollig, H. J. Strauss, L. L. Botha, and M. Esser, "Demonstration of a wavelength selected optically pumped HBr laser," in *SPIE Security+ Defence*, 2012, p. 85430E–85430E.
- [32] M. Esser, W. Koen, H. J. Strauss, C. Jacobs, L. R. Botha, and C. Bollig, "An HBr Oscillator-amplifier Pumped by a High-energy Ho: YLF Laser System," in *The European Conference on Lasers and Electro-Optics*, 2011, p. CA1\_3.
- [33] E. Lippert, H. Fonnum, and K. Stenersen, "High power multi-wavelength infrared source," in *Security + Defence*, 2010, p. 78360D–78360D.
- [34] W. S. Koen, C. Jacobs, O. Collett, and D. Esser, "Efficient Ho:YLF Laser Pumped by a Tm: fiber Laser," in *Mid-Infrared Coherent Sources*, 2013, p. MW1C–6.
- [35] I. Elder, "Thulium fibre laser pumped mid-IR source," in *SPIE Defense, Security, and Sensing*, 2009, p. 73250I–73250I.
- [36] W. Koen, C. Jacobs, L. Wu, and H. J. Strauss, "60W Ho: YLF oscillator-amplifier system," in *SPIE LASE*, 2015, p. 93421Y–93421Y.